Tellus
SERIES B
CHEMICAL
AND PHYSICAL
METEOROLOGY
PUBLISHED BY THE INTERNATIONAL METEOROLOGICAL INSTITUTE IN STOCKHOLM

Tellus (2011), 63B, 107–116

Morphology and state of mixture of atmospheric soot aggregates during the winter season over Southern Asia–a quantitative approach

By ESTHER COZ* and CAROLINE LECK, *Department of Meteorology, Stockholm University, 106 91 Stockholm, Sweden*

(Manuscript received 18 June 2010; in final form 22 September 2010)

ABSTRACT

The atmospheric brown cloud phenomena characterized by a high content of soot and a large impact on the solar radiative heating especially affects the tropical Indian Ocean during the winter season. The present study focuses on morphological characteristics and state of mixture of soot aggregates during the winter season over India. Given are quantitative measures of size, morphology and texture on aggregates collected in air at two different sites: Sinhagad near Pune in India and Hanimaadhoo in Maldives. For the latter site two different synoptic patterns prevailed: advection of air from the Arabian region and from the Indian subcontinent, respectively.

Aggregates collected at Sinhagad, were associated with open branched structures, characteristic of fresh emission and diameters between 220 and 460 nm. The Hanimaadhoo aggregates were associated with aged closed structures, smaller sizes (130–360 nm) and frequently contained inorganic inclusions. Those arriving from the Indian subcontinent were characterized by the presence of an additional organic layer that covered the aggregate structure. These organic coatings might be a reasonable explanation of the low average wash-out ratios of soot two to seven times lower than that of nss-SO_4^{2-} that have been reported for air flow arriving at Hanimaadhoo from the Indian subcontinent in winter.

1. Introduction

For global assessments of climate effects of soot (a strong absorber of light at 550 nm wavelength) global data are required, most importantly in regions where strong economic developments imply substantial increases in atmospheric concentrations, such as India, South–East Asia and China (Ramanathan et al., 2005; Foster et al., 2007).

Almost all sources of atmospheric soot are associated with combustion (Ogren and Charlson, 1983; Bond et al., 2004). The sources of soot are widely spread over the world and are mainly concentrated in highly populated areas in the tropics (Bond et al., 2004). For example, recent results over the Indian subcontinent (Gustafsson et al., 2009), based on determination of the C-14 content in soot, have shown that during the winter season (December through April) about half of the soot carried out over the Indian Ocean is derived from biomass burning rather from fossil fuel combustion.

Whereas major sources of the soot have been estimated (Gurjar et al., 2008) much less is known about the different states of soot mixture for a given mass fraction of soot. Light absorption can differ widely depending if the soot is distributed evenly over the whole volume of the collected aerosol or as a soot aggregate that has accumulated some sulfuric acid or any organic compound with active surface properties (Heintzenberg, 1978).

The composition and structure of freshly emitted soot depends to a large extent on the character of the combustion (Chakrabarty et al., 2006b; Moosmüller et al., 2009). Organic carbon (OC) can contribute from 50% to 90% of the mass (Subramanian et al., 2007; Szidat et al., 2007; Grieshop et al., 2009). Freshly emitted soot occurs as a group of hexagonal graphitic layers forming a spherule with a diameter of 10–50 nm. Some organic compounds, mainly hydrocarbons, which remain in gas phase at high temperatures during soot formation from combustion, are absorbed by the structure (Katrinak et al., 1992). Finally, the hexagonal graphitic layers generally end up in a group of primary spherules mixed with the condensed hydrocarbons in random fractal morphology (Mandelbrot, 1982; Kaye, 1994). In the atmosphere, 'fresh' soot spheres are normally aggregated together in chain-like structures that have an opened and branched structure (Smekens et al., 2007). These chain-like structures frequently present dislocations that allow the incorporation of other elements and

*Corresponding author.
e-mail: esther.coz@ciemat.es
DOI: 10.1111/j.1600-0889.2010.00513.x

basically consist of elemental and organic carbon with other elements such as oxygen, nitrogen, sulfur and hydrogen in smaller amounts (Seinfeld and Pandis, 1998). During aging in the atmosphere these structures will collapse to become a compact and closed structure. Soot originated from certain types of combustion presents a similar dense and closed structure already at emission and thus they are more resistant to atmospheric aging processes (Andreae and Gelencsér, 2006).

The structure of the primary spherules of soot, either in chain-like open structures, or in more compact and closed aggregates, will influence not only particle dispersion, transport and removal (Rogak et al., 1993; Vainshtein et al., 2004) in the atmosphere but also modify particle absorption and scattering of light (Martins et al., 1998; Fuller et al., 1999; Kalashnikova and Sokolik, 2002; Liu and Mishchenko, 2005; Liu and Mishchenko, 2007; Liu et al., 2008). It is further known that such differences in morphology (open or closed aggregates) influence water absorption and water vapour nucleation and, hence uptake in cloud droplets (Rogers et al., 1991; Pruppacher and Klett, 1997). Data on atmospheric particle morphology and quantification of how it affects all these processes are quite complex and still largely unknown. Other major questions concerning soot are the size distribution of the mixing state and the potential for transformation of the surface character of soot from hydrophobic to hydrophilic, which will in the case of cloud activation further promote a buildup of water-soluble material on the 'soot' particles, through liquid phase reactions. Together all these processes will strongly influence the estimated atmospheric lifetime of soot, which spans from a day to a month with an average of a week (Ogren and Charlson, 1983) and thus be very important for assessing its spatial distribution and radiative forcing.

The main goal of the this study is to characterize the morphology and state of mixture of soot aggregates during the winter season over the Indian subcontinent in a quantitative approach by combining Transmission Electron Microscopy (TEM) techniques with Digital Image Processing and Analysis. Electron microscopy has been previously demonstrated to be a efficient tool in the study of the heterogeneities in the structure of carbonaceous aggregates of individual particles from different sources (Katrinak et al., 1992). In this study, these techniques have been applied to ambient atmospheric aerosol samples collected at the rural Sinhagad (India) observatory and during pollutant-influenced episodes from the Indian/Arabian subcontinents at the Hanimaadhoo (Maldives) observatory.

2. The sampling sites and methods of measurements

2.1. Location and time

Samples for subsequent determinations with electron microscopy were collected at a two different locations shown in Fig. 1 (detailed information about the sampling sites can be found in Engstöm and Leck (2010)):

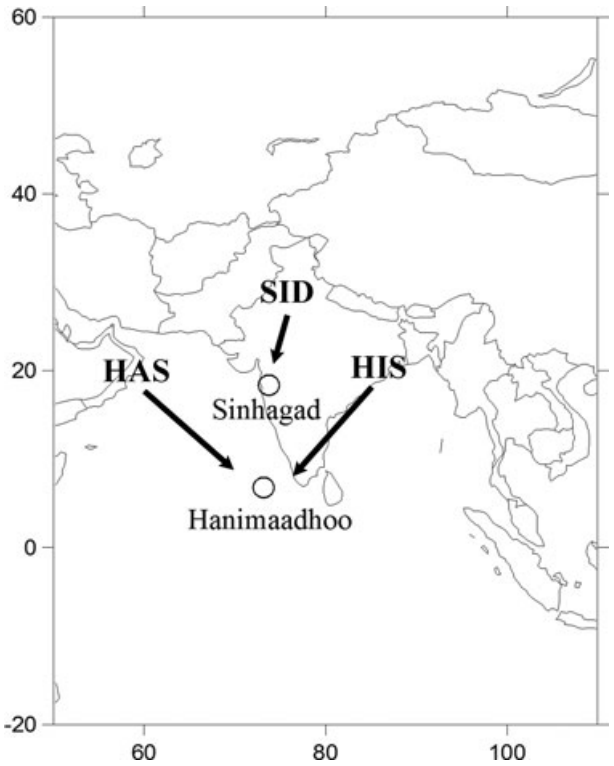

Fig. 1. Location map of the sampling sites, Hanimaadhoo and Sinhagad and corresponding trajectory clusters, Sinhagad Indian subcontinent (SID), Hanimaadhoo-Indian subcontinent (HIS) and Hanimaadhoo-Arabian Sea (HAS).

(1) Sinhagad: Meteorological observatory at Sinhagad near Pune in western India. (18° 21′ N, 73° 45′ E, 1450 m asl). There are a total of 21 samples, all of them collected during the first week of April 2006 (late winter season). The air inlet was positioned 1 meter above the roof-top at the end of a stainless steel tubing (50 mm inner diameter). The sampling tube was 4 m long and ended at the instrument inside the building.

(2) Maldives Climate Observatory Hanimaadhoo (MCOH): Meteorological observatory at Hanimaadhoo Island, 220 km from Malé in northern Maldives (6° 47′ N, 73° 11′ E, near sea level). Samples were collected at Hanimaadhoo during the month of February in both 2007 and 2008. Air was sampled from a 15 m high tower where various sensors and the inlets for air sampling were mounted. The instrument was installed at surface level in the building.

2.2. Sample collection and preparation

An electrostatic precipitator was used in sampling of the airborne particles at the two sites. Flow rate was kept very low

(10 ml min^{-1}) in order to collect particles up to about 1 μm diameter. The collection efficiency of the electrostatic precipitator used was inter-compared with the TSI 3089 Nanometer Aerosol Sampler. The collection efficiency is higher than 90% for particles smaller than 60 nm. Both instruments showed a strong agreement with a collection efficiency that fell off below 25 nm diameter.

Atmospheric aerosol particles were collected for 12 h through the take-off lines from the inlet pipe onto the surface TEM formvar-copper 3 mm grids. The grids were 'shadowed' or coated with a thin platinum film (less than 1 nm in thickness) laid down by vacuum evaporation at an angle of 26° to the surface. Its purpose is to show three-dimensional structure and to preserve a replica of particles that evaporate in the high vacuum of the microscope, or upon heating by the electron beam (mainly linked to high vacuum pressure or charging during electron beam-particle interaction). One further advantage with coating is to increase contrast to minimize errors due to losses on particle electronlucent during the subsequent digital image analysis. The drawback of the coating is that the losses on the particle electronlucent at times can hide inclusions in the microstructure. The shadowing makes the images shown in Fig. 3 resemble optical photographs in that the artificial shadows appear black and electron-absorbent material white.

2.3. Image acquisition by TEM

Imaging was performed with a Jeol JEM 2000FX, with accelerating voltage of 200 kV, Condenser aperture 2, beam spot 5 to 7. Some samples were revisited in the FEG TEM JEM2100F (Jeol) with EDS detector (Jeol) that can detect elements from atomic number 6 (C) and higher. The operation condition was then 200 kV, condenser aperture 3, beam spot size 3 to 5, Pt coated sample, windowless EDS detector, Jeol EDS program package, Digiscan CCD image system (Gatan).

3. Aggregate characterization using Digital Image Processing and Analysis

To quantitatively characterize of the structure of ambient particles it is necessary to study their size, shape, texture and phase distribution. The quantification builds on dimensionless mathematical descriptors based on Euclidean geometry, fractal geometry or textural measures of the particle shape, contour/structure and texture respectively. Table 1 gives detailed information about the aggregate structures under study. We have quantified several different mathematical descriptors (also referred to as parameters in the literature) based on the previously mentioned mathematical concepts. The degree of compactness of the soot aggregates has been quantified by four different morphological parameters, including fractal dimension. The quantification of the state of mixture, also shown in Table 1, has been characterized by three different textural parameters.

3.1. Structural descriptors: size, morphology and texture

The algorithms for the digital image processing and measurement have been introduced into a Visual Basic script in the Aphelion™ developer (ADCIS, France). The routine asks for each particle image and the particle is mathematically processed and separated from the background. Detailed information about the procedure to discriminate between particle and substrate can be found in Coz et al. (2008, 2009). Once the particle is isolated and labelled, the programmed parameters are measured. Polystyrene latex spherical particles of 60 nm diameter were used for calibration, which guaranteed deviations smaller than 5% in the measurements. However, non-perfect spherical particles, especially heavily mixed soot aggregates, may introduce artefacts in the process due to partial volatilization and shadowing. The measurement process has been checked to ensure those artefacts did not involve large errors during aggregate discrimination from the background.

Table 1. Mean, median and standard deviation of the mathematical descriptors classified by sampling site and type of transport

		Hanimaadhoo						Sinhagad		
		Arabian Sea			Indian subcontinent			Local influenced		
Mathematical descriptor		Mean	Median	Standard deviation	Mean	Median	Standard deviation	Mean	Median	Standard deviation
Size	Dp	235	230	85	245	220	120	340	350	120
Euclidean geometry	Elongation	0.38	0.37	0.20	0.37	0.35	0.20	0.57	0.63	0.22
	Convexity	0.68	0.68	0.10	0.69	0.69	0.11	0.58	0.57	0.16
	Aspect Ratio	1.57	1.51	0.32	1.57	1.48	0.35	1.88	1.86	0.48
Fractal geometry	Fractal dimension	1.60	1.60	0.23	1.62	1.64	0.22	1.42	1.40	0.22
Texture	Contrast	144	125	105	214	190	122	135	117	107
	Homogeneity	0.05	0.05	0.01	0.04	0.04	0.01	0.05	0.05	0.01
	Correlation	0.32	0.34	0.12	0.24	0.28	0.13	0.23	0.27	0.15

(a) Aggregate size: Defined as the projected sphere equivalent diameter, $D_p = 2 \cdot \sqrt{Area/\pi}$, where D_p is the equivalent diameter and the *Area* is the surface of the aggregate.

(b) Aggregate morphology: The morphological properties of the aggregates have been quantified by the following parameters:

- Elongation $= (D_{\max} - D_{\min})/(D_{\max} + D_{\min})$, where $D_{\max}$ is the longest projection of the aggregate and $D_{\min}$ is the shortest projection. Elongation is closer to zero for compact aggregates and larger than zero for open branched ones.

- Convexity $=$ Area/Area$_{\text{convex}}$, where Area$_{\text{convex}}$ is the area of the convex hull polygon. It is calculated as the ratio between the area of the particle and the area of a polygon of n sides in which the particle is inscribed (convex hull polygon). The convexity is one for perfect convex aggregates and decreases as aggregate concavity increases. This morphological property is frequently known as Solidity or Bulkiness.

- AspectRatio $= D_{\max}/D_{\min}$, where $D_{\max}$ and $D_{\min}$ are the respective longest and shortest projection of the aggregate calculated with the bounding box method (Takahama et al., 2010). This parameter was used by Adachi and Buseck (2008) to describe the chain-like structure of aggregates from Mexico City and by Chakrabarty et al. (2006a,b) to characterize aggregates emitted from spark ignition engines and from laboratory combustion of wildland fires.

- FractalDimension $= slope[\log\log plot(D_n, A_n)]$, calculated as the slope of the log–log *plot*, with $D_{\text{n}} = (1/1+(\text{n}/5))D_{\max}$ as x-axis and A_{n}, the area of the aggregate included in the circle of D_{n} diameter as y-axis. This mathematical estimation of a 2-dimensional fractal dimension is a measure of the degree of compactness of the aggregate and varies from 1 to 2, being close to 1 for open branched structures and increasing with particle compactness, being two for a perfect circle. The adjusted R^2 for the fittings for the log–log *plots* in the study is 0.99 ± 0.01. Thus, the fitting is characterized by a single slope and does not present artefacts of self-similarity (Kindratenko et al., 1994).

(c) Aggregate texture: Is in general defined as 'the arrangement or characteristics of the constituent elements present, especially in regard to surface appearance or tactile qualities. Textural analysis by image analysis quantifies some characteristic of the grey-level variation within an object. It is normally independent of object position, orientation, size, shape and brightness' (Quiang et al., 2008). The grey scale histogram of each image has been normalized to a [0, 255] brightness scale range prior to the textural analysis. The textural properties of the aggregates have been quantified by three different statistical operators (Haralick et al., 1973).

- Contrast $= \sum_{i=0}^{\max}\sum_{j=0}^{\max}(i-j)^2 P(i,j)$, being the maximum grey level in the aggregate, $P(i,j) = N(i,j)/N_{total}$ is the co-ocurrence matrix, where *N(i,j)* the number of pixel pairs *[P_1, P_2]* in which the intensity at P_1 is i and the intensity at P_2 is j and N_{total} the total number of pairs. It is a measure of the varying amount of local grey level present in the aggregate. Contrast is zero for homogenous objects and increases as local grey level variations increase.

- Homogeneity $= \sum_{i=0}^{\max}\sum_{\substack{j=0 \\ i\neq j}}^{\max} P(i,j)/(i-j)^2$. This is a measure of the aggregates textural heterogeneities. It is zero for a constant grey-level homogeneous object and increases with heterogeneity.

- Correlation $= \sum_{i=0}^{\max}\sum_{j=0}^{\max}(i-\bar{i})\cdot(j-\bar{j})\cdot P(i,j)/\sigma_i \cdot \sigma_j$, where:

$$\bar{i} = \sum_{i=0}^{\max}\sum_{j=0}^{\max} j \cdot P(i,j), \quad \bar{j} = \sum_{i=0}^{\max}\sum_{j=0}^{\max} j \cdot P(i,j)$$

$$\sigma_i^2 = \sum_{i=0}^{\max}\sum_{j=0}^{\max}(i-\bar{i})^2 \cdot P(i,j),$$

$$\sigma_j^2 = \sum_{i=0}^{\max}\sum_{j=0}^{\max}(j-\bar{j})^2 \cdot P(i,j)$$

The correlation is a measure of the grey level linear dependencies in the aggregate. Correlation is zero for perfectly homogeneous objects.

4. Morphology and state of mixture of the aggregates

4.1. Data selection

Over 300 carbonaceous aggregates collected during the dry winter season at the Sinhagad 2006 and Hanimaadhoo 2007 and 2008 observatories were quantified according to size, morphology and state of mixture.

During the dry winter season the wind patterns at Sinhagad are complex with variable directions mostly being continentally influenced. At the Hanimaadhoo observatory the mean wind is north westerly and north easterly. The former case is characterized by air influenced by mineral dust from the Middle East/Arabian peninsula transported southwards over the Arabian Sea mixed with anthropogenic-influenced aerosol particles from the Indian subcontinent and sea salt before reaching Hanimaadhoo. In the latter case, air arriving at the observatory is predominantly influenced by anthropogenic activities from the Indian subcontinent, such as combustion (Nair et al., 2005). Based on the trajectory clustering analyses performed by Engström and Leck (2010) the soot aggregates were divided into the following three clusters: 'Indian subcontinent-Sinhagad' (SID), 'Indian subcontinent–Hanimaadhoo' (HIS) and 'Arabian Sea–Hanimaadhoo' (HAS). Figure 1 shows a schematic representation of the trajectory clusters. Of the total carbonaceous aggregates collected the resulting relative number of aggregates characterized was 18% for SID and 32% HIS and 31% HAS, respectively.

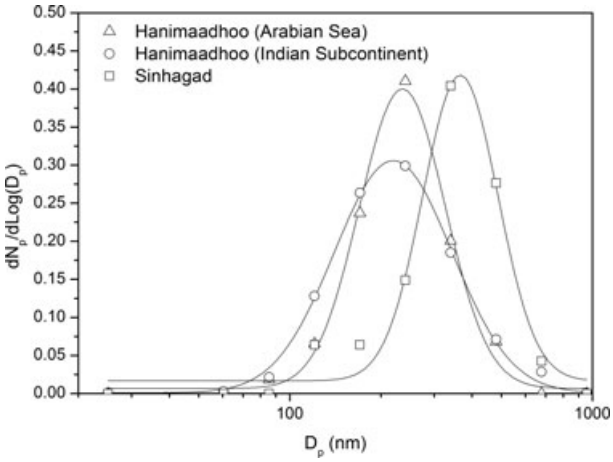

Fig. 2. Size distribution for Sinhagad, Hanimaadhoo (Indian subcontinent transport) and Hanimaadhoo (Arabian region transport). Distributions have been fitted to lognormal curves with R^2 of 0.95, 0.99 and 0.99 and peaks at 395, 270 and 260 nm, respectively.

4.2. Size distribution of the aggregates at the sites

The size distributions of the aggregates from Sinhagad, Hanimaadhoo (HIS) and Hanimaadhoo (HAS) are presented in Fig. 2. Aggregates collected at Sinhagad were larger in size (mid-diameter and standard deviation of 350 ± 120 nm) compared to the Hanimaadhoo ones [mid-diameter and standard deviation of 220 ± 120 nm (HIS) and 230 ± 85 nm (HAS)]. Aggregates size at the two sites was statistically different (*t*-Student test, $P < 0.05$). On contrary, aggregates size from the Arabian Sea and Indian subcontinent transport clusters did not differ statistically (*t*-Student test, $P > 0.05$). Despite the similarities in the mid-diameter the aggregates from the two cluster types studied at Hanimaadhoo still showed some differences in the modal width, with the HAS-cluster being more narrowly centred around the mid-diameter. In a comparison, median diameters of about 290 nm for soot containing organic and sulfate coatings have been reported Mexico City (Adachi and Buseck, 2008).

4.3. Aggregate morphology and texture

The aggregate morphological descriptors presented in Table 1 are statistically different (*t*-Student test, $P < 0.05$) for the samples collected at Hanimaadhoo and Sinhagad. The aggregates collected at the Hanimaadhoo receptor observatory presented statistically similar morphological parameters independent of type of trajectory cluster. The larger elongation and aspect ratios (AR = 1.9 ± 0.5) and smaller convexity and compactness (fractal dimension, D_f) for the Sinhagad cluster (Fig. 3a) were associated with a more open branched structure, which is typical for freshly emitted soot (Smekens et al., 2007). Resembling AR values of 2.1 ± 0.9 have been reported for Mexico city and were suggested to be associated with a not highly compacted structure for the soot aggregates (Adachi and Buseck, 2008). These

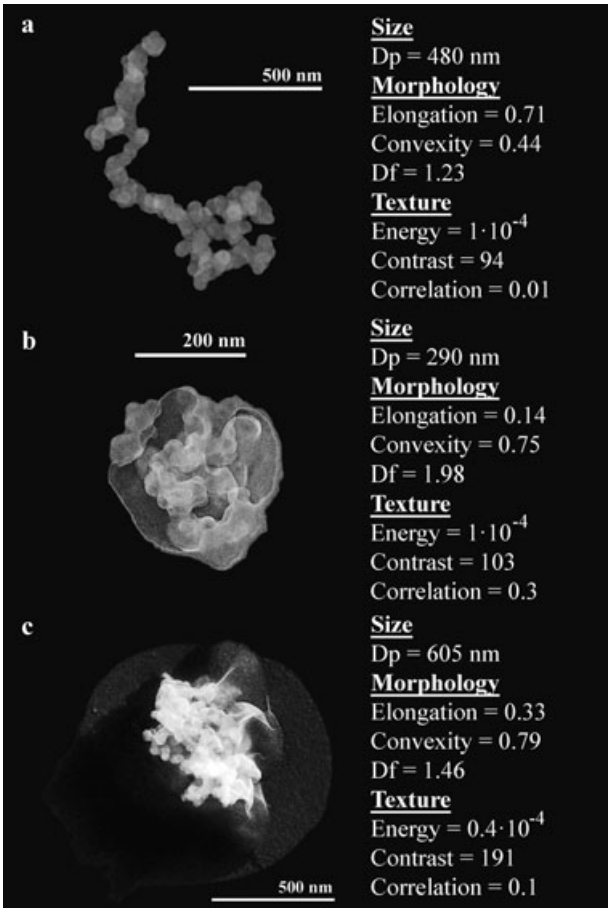

Fig. 3. Examples of the main types of agglomerates found in the samples: (a) aged agglomerate with an organic viscous film that seems to have spread out when impacting in the filter, (b) aged aggregate in an inorganic transparent kernel that frequently presents inclusions of salts in the structure and (c) fresh aggregate with very thin layer covering the structure in which the primary spherules are perfectly seen. Corresponding size, morphological and textural information can be found on the right side of each aggregate image.

types of open branches of grouped primary spherules are able to maintain the low degree of compactness in urban environments under certain conditions due to the rapid gas phase condensation of compounds forming a shell that covers the structure.

The relatively lower AR average value of 1.6 ± 0.3 determined at Hanimaadhoo, independent of the origin of the air sampled, indicated a higher degree of compactness. This is consistent with aging in the atmosphere during long-range transport where the more open branched soot structures representative of freshly emitted soot will collapse to become compact closed structures. The values for the remaining morphological descriptors, derived both of the HIS and HAS clusters, confirm the relative higher occurrence of closer and rough structures in comparison with the aggregates collected in air at the Sinhagad observatory (Fig. 3).

While the morphological parameters were appropriate for distinguishing between the degree of compactness (freshly emitted or long-range transported and aged) of the soot aggregates collected in air at the observatories, the textural parameters seem to reveal differences in uptake of other inorganic or organic compounds with implications for the light absorption of soot during transport. Contrast (C), homogeneity and correlation can be directly related to amount of grey level variability in the aggregate of study. Together with homogeneity and the presence of any self-organized structure within each aggregate the state of mixture could be revealed. These parameters were previously tested in other studies involving aerial photographs, sandstones and satellite imagery with accuracies of 82–89% during classification (Haralick et al., 1973). Other studies in geosciences that use these textural parameters are Franklin and Peddle (1987) and Cooper and Cowan (2005).

Aggregates from both the SID and the HAS cluster groups presented similar contrast and homogeneity values, whereas similar correlation values resulted for the aggregates within SID and HIS clusters (Table 1).

The result from both morphological and textural parameters together indicated a higher degree of aggregate compactness (aging) in samples associated with long-range transport in comparison with the local influenced more open branched soot structures. In addition, the textural properties were statistically different (Student's *t*-test) not only between Sinhagad and the Hannimadoo observatories but also for each of the HIS and HAS cluster group. This implies different state of mixture of the samples collected in air at the Hannimadoo receptor observatory by the uptake of inorganic and organic compounds with different properties during long-range transport from the Indian subcontinent source area.

4.4. Automated classification of the aggregates and related state of mixture

Two parameters have been used to discriminate between three different structural appearances: elongation ($E < 0.70$) and the contrast ($C < 150$) along three clusters: open-branched aggregates or fresh-like, aggregates with inorganic coating and aggregates with organic coating. Open branched structures can be recognized in distinction by the elongation ($E > 0.70$) from the other two groups ($E < 0.70$). The aggregates of this cluster display open branch structures (Fig. 3a) and have been classified as fresh-like. Aggregates with $E < 0.70$ and $C < 150$ are represented by aggregate structures covered with an inorganic bright layer (sometimes appearing inorganic inclusions), with similar characteristics to that of Fig. 3b. These particles have been classified as aggregates with inorganic coating. Aggregates with $E < 0.70$ and $C > 150$ tend to represent an organic layer that spreads out once impacted on the grid surface probably due to high viscosity associated with very low brightness when there is no presence of soot (Fig. 3c). This organic layer seems largely stable under the electron beam. These particles have been classified as aggregates with an organic coating.

Based on the applied thresholds discussed above, 12% of the aggregates fall into the fresh-like aggregates, 46% into aggregates containing inorganic inclusions and 42% into aggregates

Table 2. Particle number classification based on the state of mixture of the aggregates and the sampling location and transport process

	Cluster	Fresh-like	Inorganic layer	Organic layer
Structure	Image		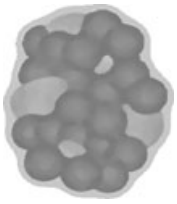	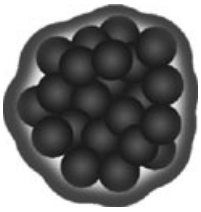
	Morphology	Open branched	Close compact	Close compact
	State of mixure	External/none	Internal inorganic inclusions/inorganic coating	Organic coating
Total		12%	46%	41%
Sinhagad	Stability	11%	4%	1%
Hanimaadhoo	AS	1%	25%	11%
	IS	1%	17%	29%
Light absorbing coefficient[a]		Increase	Decrease	Increase
Wash-out ratio[a]		Decrease	Increase	Decrease

[a] Accordingly to the results in this study combined with those in Engström and Leck (2010) and Granat et al. (2010).

with organic layers (Table 2). Making an intercomparison analysis in which the script asks the analyst to visually classify each of the aggregates based on the three defined classifications the results are 14%, 48% and 38%, respectively, which gives a more than 95% of accuracy in the automatic analysis based on the morphological and textural parameters. Within the class of fresh-like aggregates, 89% was associated with samples collected in air at Sinhagad and the other 11% in samples from Hanimaadhoo. Within the class of aggregates with inorganic inclusions, 9% was associated with Sinhagad collections and the other 91% with samples collected at Hanimmaadhoo (55% from the Arabian region and 37% from the Indian subcontinent). In the remaining class (aggregates with organic layers), 2% of the aggregates were associated with samples from Sinhagad and the other 98% from samples collected at Hanimaadhoo. The division between the HIS and HAS trajectory cluster groups was 71% and 27%, respectively. In summary, these results suggest a predominance of fresh soot structures in the SID cluster group and inorganic inclusions in both HIS and HAS clusters with a higher abundances in aggregates that arrived at the observatory from the Arabian Sea. Aggregates arriving from the Indian subcontinent showed a dominance of aggregates with an additional organic layer. Opposite to previous results reported by Spencer et al. (2008) this study suggested a differentiation in the state of mixture between aggregates collected in air sourced from the Middle-East/Arabian peninsula and transported southwards over the Arabian Sea with aggregates collected in air arriving from the Indian subcontinent before reaching Hanimaadhoo during the winter season. The implications of these differences are discussed in the next section.

5. Implications and summary

The goal of this study was to seek a better understanding of the atmospheric transformation of the light absorbing soot particles with implications for their lifetime as coagulation, vapour condensation and cloud activation all are processes expected to change the physico-chemical particle properties with ensuing consequences for climate and human health. Because of the low atmospheric concentrations of soot most analytical techniques of airborne particles are based on samples that have been enriched on matrices such as filters or impaction substrates. In situ measurements of soot light absorption require additional chemical information, namely soot morphology and state of mixture for a comprehensive analysis. As discussed above soot particles, similar to those found for Sinhagad, tends to present freshly formed particles with an open branched structure, generally associated with a hydrophobic surface with no presence of further mixture but generated during the combustion process itself (Fig. 3a). The properties of these open branched aggregates and their primary spherules with graphitic layered structure is suggested to vary with type fuel and efficiency of combustion (Schmidt-Ott, 1988; Katrinak et al., 1992; Katrinak et al., 1993; Xiong and Friedlander, 2001; Pósfai et al., 2004; Van Gilijk et al., 2004; Kis et al., 2006; Smekens et al., 2007; Sachdeva and Attri, 2008; Vernooij et al., 2009).

During long-range transport, as seen for HIS and HAS aggregates, the structure was compact with a complex internal mixture (Fig. 3a,b), dominated by inorganic inclusions and mixtures of organic/inorganic coatings for HIS and of mostly organic coatings for HAS. Thus, in addition to the differences in the structural characteristics, the difference between the two source regions and transport patterns for HIS and HAS aggregates seems to the result in different coatings. These compact close structures may attract water below saturation conditions due to capillarity condensation of water inside the porous cavities of the aggregate (Persiantseva et al., 2004; Vainshtein et al., 2004). This capillary effect is a reasonable explanation of how the hydrophobic surface of soot can start to take up not only water itself, but also gaseous reactants such as nitrogen oxides (NOx), ozone (O_3) and hydroxyl radical (OH), with subsequent chemical reactions inside the aggregate structure.

Subsequent adsorption of organic and inorganic compounds will lead to a complex system of layers over the close structure that can even hide the primary rough fractal structure of the aggregates in a subrounded film (Shi et al., 2008), which are generally associated to highly hydrophilic coatings (Johnson et al., 2005). A study in Japan Hasegawa and Ohta (2002) suggested a connection of the presence of internally mixed soot with rural environments but Johnson et al. (2005) found heavily internally mixed particles in Mexico City after less than a few hours of processing.

Aggregates size has in general been found to increase with aging in the atmosphere (Adachi and Buseck, 2008). In the specific case of this study, the meteorological scenarios seem determinant for the size of soot independently of the degree of processing of the particle. Aggregates at Hanimaadhoo were size selected during the long-range transport and present smaller sizes that those at Sinhagad. The air mass stability prevailing during the time of sampling at Sinhagad possibly favoured longer residence time of freshly emitted larger aggregates in the atmosphere without collapsing.

At Hanimadhoo the samples collected in air showed a more complex degree of closed porous structures aggregate with coatings, independent of air mass origin. Soot aggregates from Southern Ocean have been previously associated with small compact structures where large branching soot aggregates were less common (Buseck and Pósfai, 1999). The differences between the two main textural groups found in the samples were not related to an internal or external mixture, but to the properties of the coating film. Up to 60% of the aggregates in Hanimaadhoo from the Indian subcontinent origin presented this organic coating and 30% for aggregates coming from the Arabian Sea (Table 2). Two physical characteristics that distinguish this organic film from the inorganic coating is the low electrolucent

properties in the part of the structure where there is no absorbing soot and the high viscosity that makes the film spread out in the substrate (Fig. 3c).

Organic coatings have been found to alter the hygroscopic properties of soot particles in an environmental TEM study for biomass burning aggregates. Semeniuk et al. (2007b) suggested that organic coatings may complicate the deliquescence behaviour of the inorganic fraction of biomass burning particles, inhibiting the formation of deliquescence spheres. Deliquescence occurred when the inorganic phase was peripheral to the organic particle. The values and rates at which water can be incorporated into a coated particle apparently depend on the mixing state of its constituents (Semeniuk et al., 2007a,b). For instance, particles from biomass and biofuel burning, of special importance during the winter season over the Indian Ocean (Gustafsson et al., 2009), can age rapidly (Vernooij et al., 2009) and are very initially frequently associated with a largely hydrophobic behaviour with aging as a consequence of free radical polymerization of their organic molecules (Pósfai et al., 2004). In addition, recent laboratory studies reveal that certain organic coatings on black carbon can amplify the particle light absorption by 30% even with a thin coating and this amplification can be up to 100% (Shiraiwa et al., 2010).

The discussion in the previous paragraph from other studies emphasize the results in Hanimaadhoo concerned with the nature of coatings and the importance of organic coating of the original sulfate/soot mixed particles, which might have potentiated their hygroscopic behaviour and optical absorption (Table 2). The higher percentage of aggregates with organic coatings from the HIS seems to be a reasonable explanation for the higher light absorption coefficients (Engström and Leck, 2010) and smaller wash-out ratios (Granat et al., 2010) recently found during the winter season. Granat et al. (2010) found average wash-out ratios of soot from two to seven times lower than that of nss-SO_4^{2-} for winter aggregates suggesting strong hydrophobic properties that could be associated with largely externally mixed soot particles. However, according to the direct observations in the present study, the suggested hydrophobic properties of the mixtures found in this study are more probably related to the presence of organic coatings covering the soot structure.

6. Acknowledgments

We thank the MCOH staff and Lennart Granat for the help with collecting the samples. Special thanks go to Leif Bäcklin who constructed the TEM sampler designed by Keith Bigg. We are also very grateful to Agneta Öhrström for performing the TEM analyses. We specially acknowledge the funding from the International Meteorological Institute (IMI) to host Esther Coz at Stockholm University. The research was funded by the Swedish Natural Science Research Council (contract G-AA/GU 09906–316, 317; E-AD/EG 09906–315) and SIDA.

References

Adachi, K. and Buseck, P. R. 2008. Internally mixed soot, sulfates, and organic matter in aerosol particles from Mexico City. *Atmos. Chem. Phys.* **8**, 6469–6481.

Andreae, M. O. and Gelencsér, A. 2006. Black carbon or brown carbon? The nature of light-absorbing carbonaceous aerosols. *Atmos. Chem. Phys.* **6**, 3131–3148.

Bond, T. C., Streets, D. G., Yarber, K. F., Nelson, S. M., Woo, J.-H. and co-authors. 2004. A technology-based global inventory of black and organic carbon emissions from combustion. *J. Geophys. Res.* **109**, D14203, doi:10.1029/2003JD003697.

Buseck, P. R. and Pósfai, M. 1999. Airborne minerals and related aerosol particles: effects on climate and the environment. *PNAS* **96**, 3372–3379, doi:3310.1073/pnas.3396.3377.3372.

Cooper, G. R. J. and Cowan, D. R. 2005. The use of textural analysis to locate features in geophysical data. *Comput. Geosci.* **31**, 882–890.

Coz, E., Artíñano, B., Robinson, A. L., Casuccio, G. S., Lersch, T. L. and co-authors. 2008. Individual Particle Morphology and Acidity. *Aerosol Sci. Technol.* **42**, 224–232.

Coz, E., Gómez-Moreno, F. J., Pujadas, M., Casuccio, G. S., Lersch, T. L. and co-authors. 2009. Individual particle characteristics of North African dust under different long-range transport scenarios. *Atmos. Environ.* **43**, 1850–1863.

Chakrabarty, R. K., Moosmüller, H., Arnott, W. P., Garro, M. A. and Walker, J. 2006a. Structural and fractal properties of particles emitted from spark ignition engines. *Environ. Sci. Technol.* **40**, 6647–6654.

Chakrabarty, R. K., Moosmüller, H., Garro, M. A., Arnott, W. P., Walker, J. and co-authors. 2006b. Emissions from the laboratory combustion of wildland fuels: particle morphology and size. *J. Geophys. Res.* **111**, D07204.

Engström, E. and Leck, C. 2010. Reducing uncertainties associated with filter-based optical measurement of soot aerosol particles with chemical information. *Atmos. Meas. Tech. Discuss.* **3**, 1197–1227.

Foster, P., Ramaswamy, V., Artaxo, P., Berntsen, T., Betts, R. and co-authors. 2007. Changes in atmospheric constituents and in radiative forcing. In: *Climate Change 2007: The Physical Science Basis. Contribution of Working Group I to the Fourth Assessment Report of the Intergovernmental Panel on Climate Change* (eds S. Solomon, D. Qin, M. Manning, Z. Chen, M. Marquis et al.). Cambridge University Press, Cambridge, UK and New York, NY, USA.

Franklin, S. E. and Peddle, D. R. 1987. Texture analysis of digital image data using spatial cooccurrence. *Comput. Geosci.* **13**, 293–311.

Fuller, K. A., Malm, W. C. and Kreidenweis, S. M. 1999. Effects of mixing on extinction by carbonaceous particles. *J. Geophys. Res.* **104(D13)**, 15 941–15 954.

Granat, L., Engström, E., Praveen, S. and Rodhe, H. 2010. Light abssorption material ("soot") in rainwater and in aerosol particles in the Maldives. *J. Geophys. Res.*, **115**, D16307, doi:10.1029/2009JD013768.

Grieshop, A. P., Donahue, N. M. and Robinson, A. L. 2009. Laboratory investigation of photochemical oxidation of organic aerosol from wood fires 2: analysis of aerosol mass spectrometer data. *Atmos. Chem. Phys.* **9**, 2227–2240.

Gurjar, B. R., Butler, T. M., Lawrence, M. G. and Lelieveld, J. 2008. Evaluation of emissions and air quality in megacities. *Atmos. Environ.* **42**, 1593–1606.

Gustafsson, O., Krusa, M., Zencak, Z., Sheesley, R. J., Granat, L. and co-authors. 2009. Brown clouds over South Asia: Biomass or fossil fuel combustion? *Science* **323**, 495–498.

Haralick, R. M., Shanmugam, K. and Dinsein, I. 1973. Textural features for image classification. *IEEE Trans. Syst., mand Cybern.* **3**, 610–621.

Hasegawa, S. and Ohta, S. 2002. Some measurements of the mixing state of soot-containing particles at urban and non-urban sites. *Atmos. Environ.* **36**, 3899–3908.

Heintzenberg, J. 1978. Light scattering parameters of internal and external mixtures of soot and non-absorbing material in atmospheric aerosols. In: *Proceedings of the Conference on Carbonaceous Particles in the Atmosphere*, Berkley, CA (USA).

Johnson, K. S., Zuberi, B., Molina, L. T., Molina, M. J., Iedema, M. J. and co-authors. 2005. Processing of soot in an urban environment: case study from the Mexico City Metropolitan Area. *Atmos. Chem. Phys.* **5**, 3033–3043.

Kalashnikova, O. V. and Sokolik, I. N. 2002. Importance of shapes and compositions of wind-blown dust particles for remote sensing at solar wavelengths. *Geophys. Res. Lett.* **29**, 1398–1402.

Katrinak, K. A., Rez, P. and Buseck, P. R. 1992. Structural variations in individual carbonaceous particles from an urban aerosol. *Environ. Sci. Technol.* **26**, 1967–1976.

Katrinak, K. A., Rez, P., Perkes, P. R. and Buseck, P. R. 1993. Fractal geometry of carbonaceous aggregates from an urban aerosol. *Environ. Sci. Technol.* **27**, 539–547.

Kaye, B. H. 1994. *A Random Walk Through Fractal Dimensions*. VCH Verlagsgesellschaft mbH, John Wiley & Sons Inc, Weinheim, Germany.

Kindratenko, V. V., Van Espen, P. J. M., Treiger, B. A. and Van Grieken, R. E. 1994. Fractal dimensional classification of aerosol particles by computer-controlled scanning electron microscopy. *Environ. Sci. Technol.* **28**, 2197–2202.

Kis, V. K., Posfai, M. and Labar, J. L. 2006. Nanostructure of atmospheric soot particles. *Atmos. Environ.* **40**, 5533–5542.

Liu, L. and Mishchenko, M. I. 2005. Effects of aggregation on scattering and radiative properties of soot aerosols. *J. Geophys. Res.* **110**, D11211, doi:10.1029/2004JD005649.

Liu, L. and Mishchenko, M. I. 2007. Scattering and radiative properties of complex soot and soot-containing aggregate particles. *J. Quant. Spectrosc. Radiat. Transfer* **106**, 262–273.

Liu, L., Mishchenko, M. I. and Patrick Arnott, W. 2008. A study of radiative properties of fractal soot aggregates using the superposition T-matrix method. *J. Quant. Spectrosc. Radiat. Transfer* **109**, 2656–2663.

Mandelbrot, B. B. 1982. *The Fractal Geometry of Nature*. W. H. Freeman and Co, New York.

Martins, J. V., Artaxo, P., Liousse, C., Reid, J. S., Hobbs, P. V. and co-authors. 1998. Effects of black carbon content, particle size, and mixing on light absorption by aerosols from biomass burning in Brazil. *J. Geophys. Res.* **103**, 32041–32050.

Moosmüller, H., Chakrabarty, R. K. and Arnott, W. P. 2009. Aerosol light absorption and its measurement: a review. *J. Quant. Spectrosc. Radiat. Transfer* **110**, 844–878.

Nair, S. K., Parameswaran, K. and Rajeev, K. 2005. Seven year satellite observations of the mean structures and variabilities in the regional aerosol distribution over the oceanic areas around the Indian subcontinent. *Ann. Geophys.* **23**, 2011–2030.

Ogren, J. A. and Charlson, R. J. 1983. Elemental carbon in the atmosphere: cycle and lifetime. *Tellus* **35B**, 241–254.

Persiantseva, N. M., Popovicheva, O. B. and Shonija, N. K. 2004. Wetting and hydration of insoluble soot particles in the upper troposphere. *J. Environ. Monit.* **6**, 939–945.

Pósfai, M., Gelencsér, A., Simonics, R., Arató, K., Li, J. and co-authors. 2004. Atmospheric tar balls: Particles from biomass and biofuel burning. *J. Geophys. Res.* **109**, D06213, doi:06210.01029/02003JD004169.

Pruppacher, H. R. and Klett, J. D. 1997. *Microphysics of Clouds and Precipitation*.Kluwer Academic Publishers, Dordrecht.

Quiang, W., Merchant, F. and Castleman, K. R. 2008. *Microscope Image Processing*. Elsevier, Burlington, MA.

Ramanathan, V., Chung, C., Kim, D., Bettge, T., Buja, L. and co-authors. 2005. Atmospheric brown clouds: impacts on South Asian climate and hydrological cycle. *PNAS* **102**, 5326–5333

Rogak, S. N., Flagan, R. C. and Nguyen, H. V. 1993. The mobility and structure of aerosol agglomerates. *Aerosol Sci. Technol.* **18**, 25–47.

Rogers, C. F., Hudson, J. G., Hallett, J. and Penner, J. E. 1991. Cloud droplet nucleation by crude oil smoke and coagulated crude oil/wood smoke particles. *Atmos. Environ. Part A. General Topics* **25**, 2571–2580.

Sachdeva, K. and Attri, A. K. 2008. Morphological characterization of carbonaceous aggregates in soot and free fall aerosol samples. *Atmos. Environ.* **42**, 1025–1034.

Schmidt-Ott, A. 1988. In situ measurement of the fractal dimensionallity of ultrafine aerosol particles. *App. Phys. Lett.* **52**, 954–956.

Seinfeld, J. H. and Pandis, S. N. 1998. *Atmospheric Chemistry and Physics: From Air Pollution to Climate Change*. John Wiley & Sons Inc, New York.

Semeniuk, T. A., Wise, M., Martin, S., Russell, L. and Buseck, P. 2007a. Hygroscopic behavior of aerosol particles from biomass fires using environmental transmission electron microscopy. *J. Atmos. Chem.* **56**, 259–273.

Semeniuk, T. A., Wise, M. E., Martin, S. T., Russell, L. M. and Buseck, P. R. 2007b. Water uptake characteristics of individual atmospheric particles having coatings. *Atmos. Environ.* **41**, 6225–6235.

Shi, Z., Zhang, D., Ji, H., Hasegawa, S. and Hayashid, M. 2008. Modification of soot by volatile species in an urban atmosphere. *Sci. Total Environ.* **389**, 195–201, doi:110.1016/j.scitotenv.2007.1008.1016.

Shiraiwa, M., Kondo, Y., Iwamoto, T. and Kita, K. 2010. Amplification of light absorption of black carbon by organic coating. *Aerosol Sci. Technol.* **44**, 46–54.

Smekens, A., Godoi, R. H. M., Vervoort, M., Van Espen, P., Potgieter-Vermaak, S. S. and co-authors. 2007. Characterization of individual soot aggregates from different sources using image analysis. *J. Atmos. Chem.* **56**, 211–223.

Spencer, M. T., Holecek, J. C., Corrigan, C. E., Ramanathan, V. and Prather, K. A. 2008. Size-resolved chemical composition of aerosol particles during a monsoonal transition period over the Indian Ocean. *J. Geophys. Res.* **113**, D16305, doi:16310.11029/12007JD008657.

Subramanian, R., Donahue, N., Bernardo-Bricker, A., Rogge, W. and Robinson, A. L. 2007. Insights into the primary-secondary and regional-local contributions to organic aerosol and PM2.5 mass in Pittsburgh, Pennsylvania. *Atmos. Environ.* **41**, 7414–7433.

Szidat, S., Prévôt, A. S. H., Sandradewi, J., Alfarra, M. R., Synal, H.-A. and co-authors. 2007. Dominant impact of residential wood burning

on particulate matter in Alpine valleys during winter. *Geophys. Res. Lett.* **34**.

Takahama, S., Liu, S. and Russell, L. M. 2010. Coatings and clusters of carboxylic acids in carbon-containing atmospheric particles from spectromicroscopy and their implications for cloud-nucleating and optical properties. *J. Geophys. Res.* **115**, D01202, doi:10.1029/2009JD012622.

Vainshtein, P., Shapiro, M. and Gutfinger, C. 2004. Mobility of permeable aggregates: effects of shape and porosity. *J. Aerosol Sci.* **35**, 383–404.

Van Gilijk, C., J.C.M., M., Makkee, M., Molijn, J. A. and Schmidt-Ott, A. 2004. Measuring diesel soot with an scanning mobility particle sizer and electrical low pressure impactor: perfomance assessment with a model for fractal-like agglomerates. *J. Aero. Sci.* **35**, 636–655.

Vernooij, M. G. C., Mohr, M., Tzvetkov, G., Zelenay, V., Huthwelker, T. and co-authors. 2009. On Source Identification and Alteration of Single Diesel and Wood Smoke Soot Particles in the Atmosphere; An X-Ray Microspectroscopy Study. *Environ. Sci. Technol.* **43**, 5339–5344, doi: 5310.1021/es800773h.

Xiong, C. and Friedlander, S. K. 2001. Morphological properties of atmospheric aerosol aggregates. *PNAS* **98**, 11851–11856.